Macromolecules
Article
pubs.acs.org/Macromolecules

High Purity Limonene Dicarbonate as Versatile Building Block for Sustainable Non-Isocyanate Polyhydroxyurethane Thermosets and Thermoplastics

Vitalij Schimpf,[†] Benjamin S. Ritter,[†] Philippe Weis,[‡] Karsten Parison,[†] and Rolf Mülhaupt*[,†]

[†]Freiburg Materials Research Center (FMF) and Institute for Macromolecular Chemistry, University of Freiburg, Stefan-Meier-Strasse 21 and 31, 79104 Freiburg, Germany

[‡]Institute for Inorganic and Analytical Chemistry, Albertstr. 21, 79104 Freiburg, Germany

Supporting Information

ABSTRACT: Oxidation and subsequent catalytic carbonation of limonene, gained from orange peels, afford high purity limonene dicarbonate (LC) as a versatile building block for tailoring linear and cross-linked non-isocyanate polyurethanes (NIPU) from renewable resources. Spectroscopic investigations reveal so far unknown highly colored carbonation byproducts which are successfully removed to yield crystalline LC. Melt-phase polyaddition of a dimer fatty acid based diamine and its diamine-terminated LC-prepolymers with carbonated 1,4-butanediol diglycidyl ether (BDGC) produces 100% bio-based linear NIPU thermoplastics. Side-reactions occurring during polymerization account for decreasing molar mass with increasing LC content. Curing carbonated pentaerythritol glycidyl ether (PGC)/LC blends with 1,5-diaminopentane, gained from lysine, enables tailoring of 100% bio-based NIPU thermosets exhibiting unconventional property profiles. The incorporation of small amounts high purity LC substantially improves NIPU glass temperature, stiffness, and strength without sacrificing elongation at break. High purity LC prevents color formation of LC-based NIPU coatings.

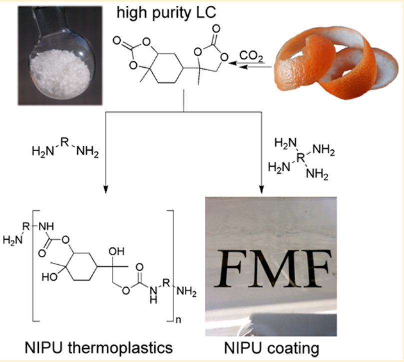

INTRODUCTION

Since the pioneering advances of Otto Bayer during the late 1940s, polyurethanes (PUs) are well-known as tailor-made materials serving the needs of highly diversified markets.[1,2] Today PUs are indispensable in daily life with applications ranging from flexible foams for bed mattresses and automotive seats to hard foams for thermal insulation, coatings for surface protection, textile fibers, adhesives, and sealants.[3] Synthetic as well as bio-based PUs are produced by polyaddition reacting isocyanate resins with polyols.[1] Going beyond the use of renewable resources such as sugars and castor oil to produce bio-based polyols, poly(propylene ether carbonate) polyols are obtained by copolymerizing CO$_2$ with propylene oxide.[4] Owing to their high toxicity and high moisture sensitivity, isocyanates require special handling and safety precautions, including careful drying of the PU formulation components. In green PU syntheses, poly(hydroxyurethane)s, termed non-isocyanate polyurethanes (NIPUs), are readily available by curing multifunctional cyclic carbonates with polyfunctional amines without requiring the use of either isocyanate or phosgene. Five-membered cyclic carbonates are widely synthesized by catalytic CO$_2$ fixation reacting epoxides with CO$_2$.[5−10] This epoxy carbonation is catalyzed by metal-centered complexes and other organocatalysts, such as tetraalkylammonium halides.[9,11−17] In order to avoid the rather expensive and elaborate separation of these catalysts, silica and polymer supported catalyst systems are employed.[9,18] Alternatively, carbonation is performed in ionic liquids or supercritical CO$_2$.[5,19,20] Also, 1,2-diols are converted into cyclic carbonates either by direct CO$_2$ fixation or via transesterification with acyclic dialkyl- or diarylcarbonates, respectively.[5] As compared to traditional PUs, poly(hydroxyurethane)s bear hydroxyl groups in their backbone.[21−24] The presence of hydroxyl groups account for enhanced hydrogen bonding, increased polarity, thermal stability, improved adhesion, and higher water uptake.[10] Unlike isocyanates, cyclic carbonates tolerate moisture and wet surfaces without causing evolution of CO$_2$ typical for the facile hydrolysis of isocyanates. Even NIPU synthesis in water is feasible.[23]

In order to improve sustainability, bio-based raw materials such as epoxidized plant oils, carbohydrates, and biopolyol glycidyl ethers have been employed in NIPU synthesis.[25−32] In this context an interesting alternative to the common NIPU syntheses exploits the Lossen rearrangement to derive thermoplastic NIPUs from ricinoleic acid.[33] Bio-based polyols, among them glycerol, pentaerythritol, and trimethylolpropane, are readily converted into bio-based epoxy resins which are carbonated and used for preparing PHU thermosets.[34] Owing to the high reactivity of terminal cyclic carbonates, glycidyl ether-derived cyclic carbonates afford fast cure which is

Received: November 13, 2016
Revised: January 5, 2017

DOI: 10.1021/acs.macromol.6b02460

Scheme 1. Synthesis of NIPU Copolymers by Advancement Reaction of Diamine-Terminated LC-Based Prepolymers Using BDGC as Chain Extender

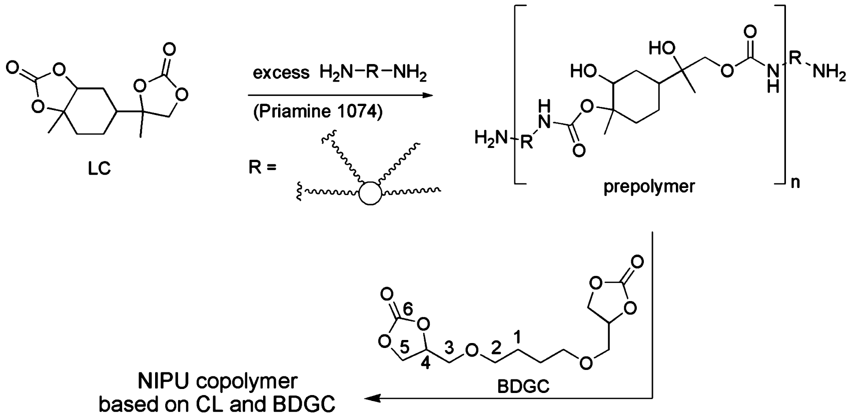

Scheme 2. Synthesis of 100% Bio-Based NIPU Thermosets from PGC/LC Blends Cured with 1,5-Diaminopentane (DAP)

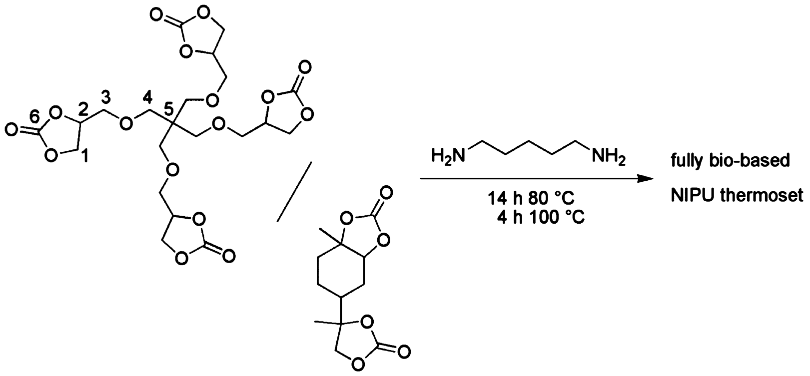

advantageous with respect to NIPU foaming.[35] Aiming at bio-based cyclic carbonates from bioresources which do not compete with food production, Bähr and Mülhaupt derived difunctional cyclic carbonates from epoxidized terpenes such as limonene.[31,36] The limonene oxidation followed by carbonation of limonene dioxide afforded limonene dicarbonate (LC) enabling the chemical fixation of 34.4 wt % CO_2. Kleij et al. produced limonene dicarbonate (LC) by carbonation of limonene dioxide in the presence of aluminum amino-triphenolate complexes and ammonium halides.[17] However, this process requires LC purification by chromatography, which is not viable in industrial production. For decades the intermediate limonene dioxide is commercially available as reactive diluent of epoxy resins.[37] Limonene monoxide was exploited as monomer to prepare linear terpene-based polycarbonates by copolymerization of limonene monoxide with CO_2.[38−41] Limonene itself is produced by more than 300 plants. In fact, (*R*)-(+)-limonene accounts for up to 97 wt % of orange peel oil, which are wastes of the orange juice production.[42−44] At present, annual limonene world production is estimated to vary between 55 000 and 85 000 tons. Main industrial limonene applications include fragrances and coatings.[45] To date, the application of limonene dicarbonate has been restricted to the formation of NIPU thermosets and low molecular weight oligomers.[31] Albeit the LC incorporation significantly improved NIPU glass transition temperature and stiffness with respect to much more flexible plant-oil-based NIPU, the highly colored liquid LC did not qualify for coating applications. Furthermore, the LC purity was insufficient for enabling the preparation of high molar mass linear NIPU thermoplastics requiring precise amine/carbonate stoichiometry. Since the early days of step growth polymerization, it is well-known that impurities and side reactions are not tolerated in such polymerizations because a slight deviation from the precise stoichiometry drastically lowers molar masses, thus rendering polymers brittle. Hence, improving the cyclic carbonate purity and preventing side reactions represents a major challenge in LC-based NIPU development, especially with respect to producing high molecular weight linear NIPU thermoplastics. Beforehand, the problem of side-reactions in NIPU formation was addressed exclusively for terminal cyclic carbonates.[46−48] No information has been available concerning side reaction occurring in LC synthesis and during LC polyaddition reactions.

Herein, we investigate the LC synthesis by carbonation of limonene dioxide in order to identify and remove LC impurities, aiming at preventing both color formation and NIPU molar mass losses encountered in LC polyaddition. In a model study LC is reacted with 1-octylamine in order to facilitate the spectroscopic analysis of the reaction products. Diamine-terminated NIPU prepolymers are prepared by nonstoichiometric polyaddition of LC with excess of flexible diamine (Priamine 1074), abbreviated as PA, which is commercially available and obtained by hydrogenation of dimer fatty acid diamides. The influence of LC regarding the molecular weight and the thermal properties of thermoplastic NIPU-copolymers is studied. In solvent-free melt-phase polyaddition, LC-based NIPU prepolymers are chain-extended by polyaddition with highly reactive difunctional carbonated

1,4-butanediol diglycidyl ether, abbreviated as BDGC (see Scheme 1).

Moreover, as is illustrated in Scheme 2, high purity LC is blended together with polyfunctional carbonated pentaerythritol glycidyl ether (PGC) in order to examine the influence of the LC incorporation on the thermal and mechanical properties of 100% bio-based NIPU obtained by curing the LC/PGC blend with bio-based 1,5-diaminopentane (DAP) derived from lysine by decarboxylation. Bio-based PGC is obtained by carbonation of the bio-based glycidyl ether prepared from epichlorohydrin, derived from glycerol, and pentaerythritol, like Perstorp's Voxtar M100, which is produced from formaldehyde and acetaldehyde derived from renewable resources. Both aldehydes can be produced from oxidation of the respective bio-based alcohols.[49]

■ EXPERIMENTAL SECTION

Materials. 1,4-Butanediol diglycidyl ether (technical grade, ERISYSTM GE-21, EEW = 128 g/equiv) and Priamine 1074 (amine value from titration: 210 mg KOH/g) were kindly provided by CVC emerald materials and Croda, respectively. Limonene dioxide (mixture of *cis*-(+) and *trans*-(+) isomers) was obtained from Rheinmetall Nitrochemie. Carbon dioxide grade N45 was supplied by Air Liquide. Octylamine (99%) and TBAB (≥99%) were purchased from Sigma-Aldrich. Pentaerythritol glycidyl ether (technical grade, ipox CL 16, EEW = 161 g/equiv) was kindly provided by ipox chemicals. Lupasol FG (M_n = 800 g/mol) and 1,5-diaminopentane were kindly provided by BASF.

Methods. NMR spectra were recorded on an ARX 300 spectrometer from Bruker at room temperature. The chemical shifts were referenced to the solvent signals. For FT-IR spectroscopy a Bruker FT-IR Vector 2200 with attached Goldengate unit was available. The spectra were recorded from the solid plaques using attenuated total reflectance (ATR) technique. Up to 20 scans were superposed to create the final spectra with a resolution of 4 cm^{-1} in the range from 800 to 4000 cm^{-1}. SEC measurements were performed in *N*,*N*-dimethylacetamide on a PSS Agilent 1200 Series with connected refractive index detector. For separation at room temperature SDV columns (5 μm; 100, 1000, and 10 000 Å) were used. The calibration was carried out with poly(methyl methacrylate). DSC measurements were performed on a PerkinElmer Pyris 1 with a heating and cooling rate of 10 K/min. Data reported are from second heating cycles if not otherwise indicated. A PerkinElmer Pyris TGA 4000 was used for the thermogravimetric analysis. The sample was heated under air from 50 up to 650 °C with a heating rate of 10 K/min. Mass spectra were obtained using an Exactive mass spectrometer from Thermo Scientific in atmospheric pressure chemical ionization mode (APCI). Methanol served as solvent (may cause monomer−$MeOH_2^+$ adducts). Vaporization temperatures were 150 °C (for LC and impure LC) or 200 °C (for model reaction). An assist gas was used and led through an ammonium acetate solution prior to measurement. The latter may cause monomer−NH_4^+ adducts. Elemental analysis was performed on a VarioEL from Elementaranalysensysteme GmbH. Gloss was measured on an Erichsen Picogloss 650 MC (60°, statistical average of ten single measurements). DMA measurements were performed on a Q800 from TA Instruments. Every sample was cooled down to −40 °C, the temperature was held for 5 min, and afterward the sample was heated up with 3 K min^{-1}. The specimens were in the shape of a rectangle with the dimensions of 80 mm × 12 mm × 3 mm. Deformation was 0.1%, and the frequency amounted 1 Hz. The glass transition was determined from the maximum of the tan δ curve.

Tensile testing was performed on a Zwick Z005 (Ulm, Germany, ISO 527−1/2) with a drawing speed of 5 mm/min. The mechanical properties such as elastic modulus, tensile strength and breaking elongation extracted from measurements at room temperature by taking the statistical average of at least five test specimens (5A). Single-crystal X-ray diffraction measurements were performed on a Bruker Smart Apex II Quazar diffractometer. A suitable crystal was selected and mounted in perfluorinated alkyl ether oil on a MiTeGen Micromount and then introduced into the machine. The crystal was kept at 100(2) K during data collection. The frames were integrated with the SAIN software package (V8.34A, Bruker AXS, Madison, WI, 2015). Data were corrected for absorption effects using the SADABS[50] program (empirical multiscan method). The structure was solved with the ShelXT[51] structure solution program using Direct Methods and refined with the ShelXL[52] refinement package using the ShelXle gui[53] by least-squares minimization with anisotropic thermal parameters for all atoms. The hydrogen atoms were added with HFIX instructions. One disagreeable reflection was removed using the OMIT command. The absolute structure was determined using the Parsons method.[54] CCDC 1498361 contains the supplementary crystallographic data for this paper. This data can be obtained free of charge via http://www.ccdc.cam.ac.uk/products/csd/request/ (or from Cambridge Crystallographic Data Centre, 12 Union Road, Cambridge, CB2 1EZ, UK (fax: ++44-1223-336-033; e-mail: deposit@ccdc.cam.ac.uk).

Synthesis of Carbonated 1,4-Butandiol Diglycidyl Ether (BDGC). Technical grade 1,4-butanediol diglycidyl ether was distilled (982.3 g, $T_{0.6-0.9\ \mathrm{mbar}}$ = 105−112 °C) to separate the diglycidyl ether from higher molecular weight side products. The distillate (498.5 g) shows remaining monoglycidyl ether (25 mol %, determined by ^1H NMR) as the only side product left due to similar boiling points. The carbonation of the distillate was carried out in a stainless steel reactor (485.3 g, 4.429 mol of epoxy groups, 1.661 mol of dimer, 130 °C, 30 bar of CO_2, 26 h) with TBAB as catalyst (4.9 g, 15 mmol, 1 wt %). The product was received as a colorless low-viscosity liquid, and the pure carbonated butanediol diglycidyl ether (BDGC) was precipitated from ethyl acetate (0.5 mL/g, at 10 °C, overnight), dried in a vacuum oven (60 °C, 1 mbar, 24 h), and received as a white powder (353.4 g, 1.217 mol, 73%); mp 80 °C. ΔH_m = 99 J/g; T_d = 281 °C. ^1H NMR (299.87 MHz, $CDCl_3$): δ = 1.63 (4H, 1-CH_2), 3.50−3.70 (8H, 2-CH_2, 3-CH_2), 4.35−4.51 (4H, 5-CH_2,), 4.80 (2H, 4-CH,) ppm. ^{13}C NMR (75.41 MHz, $CDCl_3$): δ = 26.2 (1-C), 66.32 (5-C), 69.7 (3-C), 71.7 (2-C), 75.3 (4-C), 155.2 (6-C) ppm. FTIR (ATR): $\tilde{\nu}_{max}$ = 2928−2869 (C−H), 1780 (C═O, 5mcc), 1396, 1133, 1046 (C−O), 1002 (C−O) cm^{-1}.

Synthesis of Limonene Dicarbonate (LC). The carbonation of limonene dioxide was carried out, analogous to literature,[31] in a stainless steel reactor (1506 g, 8.951 mol, 135 °C, 30 bar of CO_2, 4 days) with TBAB as catalyst (30.1 g, 93.4 mmol, 2 wt %), and the product was received as a brown viscous liquid. Impure-LC: ^1H NMR (299.87 MHz, $CDCl_3$): δ = 1.01−2.50 (m), 3.32 (m, 2H, $^+N{-}CH_2{-}$, TBAB), 4.05−4.50 (m, 1-CH, 2/2′-CH_2), 4.79 (m, 1H, 4/4′-CH_2), 4.82 (m, 1H, 5/5′-CH_2), 4.87 (m, 1H, 4/4′-CH_2), 4.99 (m, 1H, 5/5′-CH_2), 5.22, 5.45, 5.56 (m, 1H, 3-CH) ppm. MS (APCI): *m*/*z*: 93.070, 133.101 [(F-4H_2O)-H^+], 151.112 [(F-3H_2O)-H^+], 230.139 [B/C/D/E/F-NH_4^+], 274.128 [A-NH_4^+], 289.128 [A-$MeOH_2^+$]. Elemental analysis: calcd for $C_{12}H_{16}O_6$ (256.25): C: 56.25, H: 6.29. Found: C: 60.25, H: 7.27.

The viscous liquid was diluted with ethyl acetate (500 mL) and crystalline LC precipitated (517 g, 2.02 mol, 23%) when adding triethylamine (1150 mL). The white precipitate still showed minor TBAB and olefinic signals in the ^1H NMR spectrum and therefore was recrystallized from isohexane/ethyl acetate (v:v, 9:1, ∼0.8 mL/g LC). The mother liquor and washing liquids were collected, the solvent was evaporated under reduced pressure, and the residues were recrystallized as before. That process was repeated one more time. Then all the crystallites were collected and yielded a blend of two stereoisomers with no further impurities (415 g, 1.62 mol, 18%). The ratio of cis:trans was determined to be 2:3 using the two signals in the ^1H NMR spectrum in the range between 2.0 and 2.4 ppm. All further experiments were done with this stereoisomer blend if not otherwise indicated. LC-blend: mp 122/157 °C, ΔH_{m1} = 90 J/g (from first heating curve); T_d = 340 °C. ^1H NMR (299.87 MHz, $CDCl_3$): δ = 1.25−1.40 (m, 2H), 1.44−1.45 (3× s, 6H), 1.57−1.80 (m, 3H), 2.07−2.16 (m, 0.62H), 2.27−2.34 (m, 1.41H), 4.09 (d, ^2J = 8.7 Hz, 1H, $-O_2CO{-}CH_2$), 4.26 (d, ^2J = 8.7 Hz, 1H, $-O_2CO{-}CH_2$), 4.40 (2× dd, ^3J = 9.1/6.7 Hz and ^3J = 9.0/6.8 Hz, 1H, $-O_2CO{-}CH$). ^{13}C NMR

(75.41 MHz, $CDCl_3$): δ = 20.7, 20.9, 21.0, 21.4, 26.0, 29.0, 32.4, 32.5, 40.5, 40.6, 73.0, 73.2, 79.6, 79.7, 82.0, 82.1, 84.7, 84.8, 154.1, 154.2, 154.2, 154.3 ppm. FTIR (ATR): $\tilde{\nu}_{max}$ = 2984−2938 (C−H), 1779 (C═O, 5mcc), 1249, 1140, 1066 (C−O), 1022 (C−O) cm^{-1}. MS (APCI): *m*/*z*: 257.102 [A-H^+], 274.128 [A-NH_4^+], 289.128 [A-$MeOH_2^+$]. Elemental analysis: calcd for $C_{12}H_{16}O_6$ (256.25): C: 56.25, H: 6.29. Found: C: 56.22, H: 6.26.

Upon second recrystallization (173.4 g of the isomer blend, 676.7 mmol) with isohexane/ethyl acetate (v:v, 20:1, ∼0.6 mL/g LC) specifically one stereoisomer (*trans*-LC) crystallized (25.3 g, 98.7 mmol). The increased amount of ethyl acetate, which is a good solvent for LC, allows under these conditions only the crystallization of the isomer with the better disposition for crystallizing. *trans*-LC: mp 165 °C, ΔH_{m1} = 88 J/g (from first heating curve). ^1H NMR (299.87 MHz, $CDCl_3$): δ = 1.25−1.40 (m, 2H), 1.45/1.46 (2× s, 6H), 1.57−1.80 (m, 3H), 2.07−2.16 (m, 1H), 2.28−2.36 (m, 1H), 4.09 (d, ^2J = 8.7 Hz, 1H, $-O_2CO-CH_2$), 4.27 (d, ^2J = 8.7 Hz, 1H, $-O_2CO-CH_2$), 4.39 (dd, ^3J = 9.1/6.8 Hz, 1H, $-O_2CO-CH$) ppm. ^{13}C NMR (75.41 MHz, $CDCl_3$): δ = 20.7, 20.9, 21.0, 21.4, 26.0, 29.0, 32.4, 32.5, 40.5, 40.6, 73.0, 73.2, 79.6, 79.7, 82.0, 82.1, 84.7, 84.8, 154.1, 154.2, 154.2, 154.3 ppm. FTIR (ATR): $\tilde{\nu}_{max}$ = 2984−2938 (C−H), 1779 (C═O, 5mcc), 1249, 1140, 1066 (C−O), 1022 (C−O) cm¯1. Crystal data for $C_{12}H_{16}O_6$ (*trans*-LC) (CCDC 1498361) (*M* = 256.25 g/mol): orthorhombic, space group $P2_12_12_1$ (no. 19), *a* = 8.1730(3) Å, *b* = 10.8726(4) Å, *c* = 13.4157(5) Å, *V* = 1192.14(8) $Å^3$, *Z* = 4, *T* = 100(2) K, μ(Mo Kα) = 0.115 mm^{-1}, D_{calc} = 1.428 g/cm^3, 95 560 reflections measured (4.822° ≤ 2Θ ≤ 62.132°), 3569 unique (R_{int} = 0.0262, R_{sigma} = 0.0106) which were used in all calculations. The final R_1 was 0.0268 ($I > 2\sigma(I)$), and wR_2 was 0.0726 (all data).

Preparation of LC-Based NIPU Prepolymers. Ground (with common mortar and pestle) LC was mixed with a predefined excess of PA inside a 100 mL round-bottom flask and stirred (using a mechanical "KPG" stirrer) at elevated temperature and under a nitrogen atmosphere until complete turnover of cyclic carbonate groups was observed in the IR spectrum. The Supporting Information contains a list with exact weight portions and respective reaction conditions (Table S1).

Prepol-1: FTIR (ATR): $\tilde{\nu}_{max}$ = 2923 (C−H), 2850 (C−H), 1703 (C═, urethane), 1464 cm^{-1}.

Prepol-2: FTIR (ATR): $\tilde{\nu}_{max}$ = 3317 (N−H, O−H), 2921 (C−H), 2850 (C−H), 1699 (C═O, urethane), 1539, 1459, 1250, 1067 (C−O), 1139, 1016 (C−O) cm^{-1}.

Prepol-3: FTIR (ATR): $\tilde{\nu}_{max}$ = 3333 (N−H, O−H), 2925 (C−H), 2852 (C−H), 1697 (C═O, urethane), 1541, 1459, 1247, 1067 (C−O), 1145, 1013 (C−O) cm^{-1}.

Preparation of Linear NIPU. The cyclic carbonate (LC or BDGC) was added to the respective amine (PA, Prepol-1, Prepol-2, or Prepol-3) inside a 100 mL round-bottom flask and stirred (using a mechanical "KPG" stirrer) at elevated temperature and under a nitrogen atmosphere. The Supporting Information contains a list with exact weight portions and respective reaction conditions (Tables S2 and S3) as well as NMR spectra (Figures S7−S11, S19, and S20).

BDGC_PA: T_g = −18 °C; T_d = 300 °C. FTIR (ATR): $\tilde{\nu}_{max}$ = 3333 (N−H, O−H), 2919 (C−H), 2851 (C−H), 1696 (C═O, urethane), 1539, 1464, 1253, 1115, 1050 (C−O) cm^{-1}. SEC (DMAc, PMMA standard): M_n = 22.1 kg mol^{-1}, M_w = 46.7 kg mol^{-1}, PDI = 2.1.

BDGC^3-LC^1_PA: T_g = −10 °C; T_d = 277 °C. FTIR (ATR): $\tilde{\nu}_{max}$ = 3331 (N−H, O−H), 2922 (C−H), 2852 (C−H), 1795 (C═O, 5mcc), 1696 (C═O, urethane), 1540, 1457, 1253, 1116, 1052 (C−O) cm^{-1}. SEC (DMAc, PMMA standard): M_n = 12.1 kg mol^{-1}, M_w = 26.5 kg mol^{-1}, PDI = 2.2.

BDGC^1-LC^1_PA: T_g = −1 °C; T_d = 282 °C. FTIR (ATR): $\tilde{\nu}_{max}$ = 3333 (N−H, O−H), 2921 (C−H), 2852 (C−H), 1793 (C═O, 5mcc), 1695 (C═O, urethane), 1535, 1457, 1254, 1115, 1047(C−O) cm^{-1}. SEC (DMAc, PMMA standard): M_n = 10.7 kg mol^{-1}, M_w = 21.8 kg mol^{-1}, PDI = 2.0.

BDGC^2-LC^3_PA: T_g = 5 °C; T_d = 291 °C. FTIR (ATR): $\tilde{\nu}_{max}$ = 3320 (N−H, O−H), 2921 (C−H), 2852 (C−H), 1800 (C═O, 5mcc), 1697 (C═O, urethane), 1535, 1461, 1250, 1133, 1050 (C−O) cm^{-1}. SEC (DMAc, PMMA standard): M_n = 10.6 kg mol^{-1}, M_w = 22.8 kg mol^{-1}, PDI = 2.1.

LC_PA: T_g = −12 °C; T_d = 281 °C. FTIR (ATR): $\tilde{\nu}_{max}$ = 3322 (N−H, O−H), 2924 (C−H), 2851 (C−H), 1801 (C═O, 5mcc), 1696 (C═O, urethane), 1639, 1542, 1461, 1263, 1132, 1034 (C−O) cm^{-1}. SEC (DMAc, PMMA standard): M_n = 4.3 kg mol^{-1}, M_w = 8.1 kg mol^{-1}, PDI = 1.9.

Model Reaction LC_OA. LC (2.015 g, 7.863 mmol) and octylamine (2.60 mL, 2.03 g, 15.7 mmol) were dissolved in chloroform (20 mL) and refluxed for 4 days under a nitrogen atmosphere. Afterward chloroform was removed under reduced pressure. ^1H NMR (299.87 MHz, $CDCl_3$): δ = 0.85 ($-CH_3$), 1.0−1.7, 1.8, 2.2−2.4, 2.66 ($-CH_2NH_2$), 3.12 ($-CH_2NHC({=}O)O-$), 3.29−3.34, 3.91- 4.09, 4.29−4.35 ($-O_2CO-CH$), 4.55, 5.00 (−OH) ppm. ^{13}C NMR (75.41 MHz, $CDCl_3$): δ = 14.2, 20.4, 20.7, 21.0, 21.3, 21.7, 22.0, 22.3, 22.7, 26.1, 26.9, 27.0, 27.5, 28.8, 29.3, 29.4, 29.5, 30.0, 31.4, 31.9, 32.2, 33.1, 33.6, 36.9, 37.1, 39.5, 39.8, 41.2, 41.3, 42., 44.0, 70.1, 70.4, 70.6, 73.0, 73.1, 73.2, 73.3, 76.1, 76.3, 80.8, 81.0, 82.3, 82.4, 83.3, 83.5, 154.8, 156.1, 156.9, 157.1 ppm.

Synthesis of Carbonated Pentaerythritol Glycidyl Ether (PGC). The carbonation of pentaerythritol glycidyl ether (1233.4 g, 3.422 mol of epoxy groups) was carried out in a stainless steel reactor (120 °C, 30 bar CO_2, 1 wt % TBAB, 40 h). The product was degassed in a vacuum oven and then used without further purification. The cyclic carbonate value was determined from the epoxy equivalent of the starting material assuming 100% conversion and with ^1H NMR spectroscopy using naphthalene as internal standard. The calculation is given in the Supporting Information (p S3) and yielded a carbonate value of CV = (4.9 ± 0.1) mmol g^{-1}. ^1H NMR (299.87 MHz, $CDCl_3$): δ = 3.38−3.95 (m, 3-CH_2, 4-CH_2), 4.33−4.56 (m, 2H, 1-CH_2), 4.82 (m, 1H, 2-CH) ppm. FTIR (ATR): $\tilde{\nu}_{max}$ = 2971−2865 (C−H), 1783 (C═O, 5mcc), 1478, 1395, 1361, 1334, 1167, 1126, 1103, 1084, 1073 (C−O), 1043 (C−O) cm^{-1}.

Preparation of NIPU Thermosets. Prior to use, the LC was grinded using a laboratory mortar and pestle. Mixtures of PGC and LC were prepared with 10, 20, 30, and 50 wt % LC. The heterogeneous mixture was stirred in a beaker using a spatula at elevated temperature (130 °C, ∼30 min) until all LC dissolved in PGC. The homogeneous cyclic carbonate blends remained in all cases clear after cooling to room temperature as no LC crystallization could occur. The four carbonate mixtures, as well as the neat PGC, were each heated to 100 °C, then the respective amount of 1,5-diaminopentane (DAP) was added, and the mixture stirred for 30−50 s using a mechanical "KPG" stirrer with 2000 rpm before pouring into a heated alumina mold (80 °C). The curing was performed in an oven (16 h at 80 °C, 4 h at 100 °C). The Supporting Information contains a list with exact weight portions and respective reaction conditions (p S2, Tables S4 and S5).

PGC_DAP: T_g = 41 °C. FTIR (ATR): $\tilde{\nu}_{max}$ = 3324 (N−H, O−H), 2924 (C−H), 2867 (C−H), 1795 (C═O, 5mcc), 1694 (C═O, urethane), 1532, 1455, 1245, 1093 (C−O), 1043 (C−O) cm^{-1}.

PGC_10LC_DAP: T_g = 45 °C. FTIR (ATR): $\tilde{\nu}_{max}$ = 3308 (N−H, O−H), 2930 (C−H), 2873 (C−H), 1789 (C═O, 5mcc), 1692 (C═O, urethane), 1532, 1455, 1248, 1091 (C−O), 1030 (C−O) cm^{-1}.

PGC_20LC_DAP: T_g = 48 °C. FTIR (ATR): $\tilde{\nu}_{max}$ = 3306 (N−H, O−H), 2933 (C−H), 2871 (C−H), 1787 (C═O, 5mcc), 1692 (C═O, urethane), 1530, 1461, 1247, 1094 (C−O), 1030 (C−O) cm^{-1}.

PGC_30LC_DAP: T_g = 58 °C. FTIR (ATR): $\tilde{\nu}_{max}$ = 3324 (N−H, O−H), 2930 (C−H), 2864 (C−H), 1791 (C═O, 5mcc), 1696 (C═O, urethane), 1526, 1453, 1250, 1095 (C−O), 1026 (C−O) cm^{-1}.

PGC_50LC_DAP: T_g = 62 °C. FTIR (ATR): $\tilde{\nu}_{max}$ = 3311 (N−H, O−H), 2934 (C−H), 2871 (C−H), 1790 (C═O, 5mcc), 1692 (C═O, urethane), 1526, 1459, 1249, 1099 (C−O), 1026 (C−O) cm^{-1}.

Preparation of LC_PEI. Prior to use the LC was grinded using a laboratory mortar and pestle. LC (12.641 g, 98.663 mmol of "CO_3") was heated inside a beaker (160 °C) until all the crystallites were melted. PEI (9.664 g, 99.06 mmol of "NH_2") was heated inside a syringe (100 °C) and added to the still hot LC. The mixture was stirred for 45 s without any external heating using a mechanical "KPG" stirrer with 2000 rpm before pouring into a heated alumina mold (100 °C). The curing was performed in an oven (16 h at 100 °C). FTIR

(ATR): $\tilde{\nu}_{max}$ = 3310, 2930, 2839, 1797 (C═O, 5mcc), 1694 (C═O, urethane), 1528 (N−H), 1452, 1371, 1257, 1115, 1056 (C−O), 1021 (C−O) cm^{-1}.

Preparation of LC_PEI Coating. Prior to use, the LC was grinded using a laboratory mortar and pestle. LC (3.406 g, 26.584 mmol of "CO_3") was heated inside a beaker (160 °C) until all the crystallites were melted. PEI (2.667 g, 27.34 mmol of "NH_2") was heated inside a syringe (100 °C) and added to the still hot LC. The mixture was stirred for 40 s without any external heating using a mechanical "KPG" stirrer with 2000 rpm before pouring onto a heated glass plate (100 °C). A doctor blade with an adjusted 0.5 mm gap was used to produce a thin coating of the reaction mixture on the glass. The curing was then performed in an oven (16 h at 100 °C). Measured gloss: 140 ± 5.

Preparation of Impure-LC_PEI. Liquid, impure LC (11.940 g), as received from the reactor and so far used in the literature for NIPU preparation, was heated inside a beaker (90 °C). PEI (9.089 g, 93.16 mmol of "NH_2") was heated inside a syringe (90 °C) and added to the still hot LC. The mixture was stirred for 45 s without any external heating using a mechanical "KPG" stirrer with 2000 rpm before pouring into a heated alumina mold (80 °C). The curing was performed in an oven (16 h at 100 °C). A mechanical characterization was not possible as the resulting tensile testing samples tuned out to be too brittle to be measured. FTIR (ATR): $\tilde{\nu}_{max}$ = 3296, 2930, 2825, 1797 (C═O, 5mcc), 1696 (C═O, urethane), 1530 (N−H), 1451, 1371, 1257, 1115, 1036 (C−O) cm^{-1}.

■ RESULTS AND DISCUSSION

High-Purity Limonene Dicarbonate (LC). The solvent-free carbonation of limonene dioxide (mixture of *cis*-(+) and *trans*-(+) isomers) was performed in bulk at 135 °C by reacting limonene dioxide with CO_2 at 30 bar CO_2 pressure in the presence of 2 wt % tetrabutylammonium bromide (TBAB) over the period of 4 days to afford LC as a highly colored brownish viscous liquid. The turnover of epoxy groups was monitored with ^{1}H NMR spectroscopy. In the past this colored crude LC (see Figure 1, left) was used for the preparation of linear NIPU and NIPU thermosets without further purification or purified only by extracting TBAB residues.[31]

Figure 1. LC before (left) and after purification by crystallization (right).

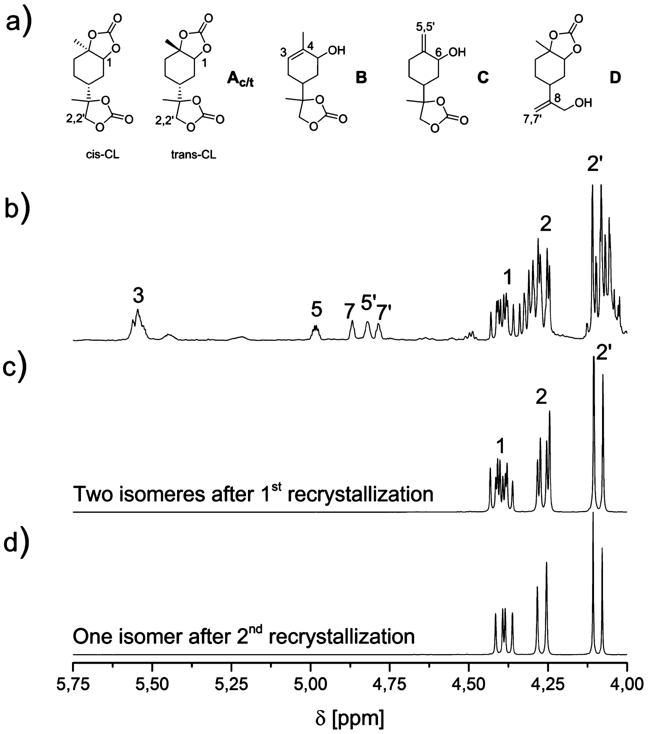

Figure 2. (a) Main ($\mathbf{A}_{c/t}$) and side products (**B**, **C**, **D**) in LC synthesis via TBAB-catalyzed CO_2 fixation with limonene dioxide. (b) ^{1}H NMR spectrum ($CDCl_3$) of unpurified LC. (c) ^{1}H NMR spectra ($CDCl_3$) of a *cis*/*trans*-LC blend (cis:trans = 2:3) obtained after first recrystallization. (d) ^{1}H NMR spectra ($CDCl_3$) of isomerically pure *trans*-LC obtained after second recrystallization.

The ^{1}H NMR spectrum of the crude reaction product, displayed in Figure 2, shows various signals in the range of 4.6−5.6 ppm that couple with ^{13}C atoms in the range between 105 and 150 ppm and thereby indicates the existence of olefinic groups. According to literature, in the first step of catalytic carbonation, the nucleophilic attack of bromide from TBAB at the epoxy ring causes ring-opening to produce highly reactive bromo alkoxides.[5,13] Preferably, bromoalkoxides react with CO_2 to form 5-membered cyclic carbonate (*cis*- and *trans*-LC displayed in Figure 2a), thus regenerating the TBAB catalyst by splitting off bromide during ring closure. However, to date, the competing side reaction and olefin byproduct formation was ignored. In principle, as illustrated in Figures 2 and 3, bromide elimination prior to the CO_2 fixation affords olefinic groups and alcohols as side products which do not react with CO_2 (see Figures 2 and 3, **B** to **E**). The presence of olefinic groups was confirmed by two-dimensional NMR spectroscopy (Figure S14) and by mass spectrometry (m/z = 230.139 [B/C/D/E/F-NH_4^+]; Figure S79). It should be noted that the *α*,*β*-unsaturated alcohol derived from the exocyclic carbonate readily tautomerizes to form the corresponding aldehyde in quantitative yield (see Figure 3, **E**).

On dilution with ethyl acetate and addition of triethylamine, LC crystallization removed TBAB as well as most olefin and aldehyde byproducts to form a LC stereoisomer blend of *cis*- and *trans*-LC (see $\mathbf{A}_{c/t}$ in Figure 2a). According to the ^{1}H NMR spectra, this precipitated LC still contained around 5% impurities. Therefore, it was recrystallized from isohexane/ethyl acetate. The resulting high purity of the recrystallized LC-blend (cis:trans = 2:3) was confirmed by NMR spectroscopy (Figures S4 and S15), elemental analysis, and mass spectrometry (Figure S78). The second recrystallization with higher amount of ethyl acetate in the solvent mixture led to the exclusive crystallization of one isomer. Kleij et al. studied highly active catalysts for the chemical fixation of CO_2 with epoxides in the presence of Al(aminotriphenolate) complexes combined with ammonium halides.[55] In a recent publication they applied their catalyst systems for the carbonation of limonene dioxide at 85 °C and at 120 °C and employed chromatography for

DOI: 10.1021/acs.macromol.6b02460
Macromolecules XXXX, XXX, XXX−XXX

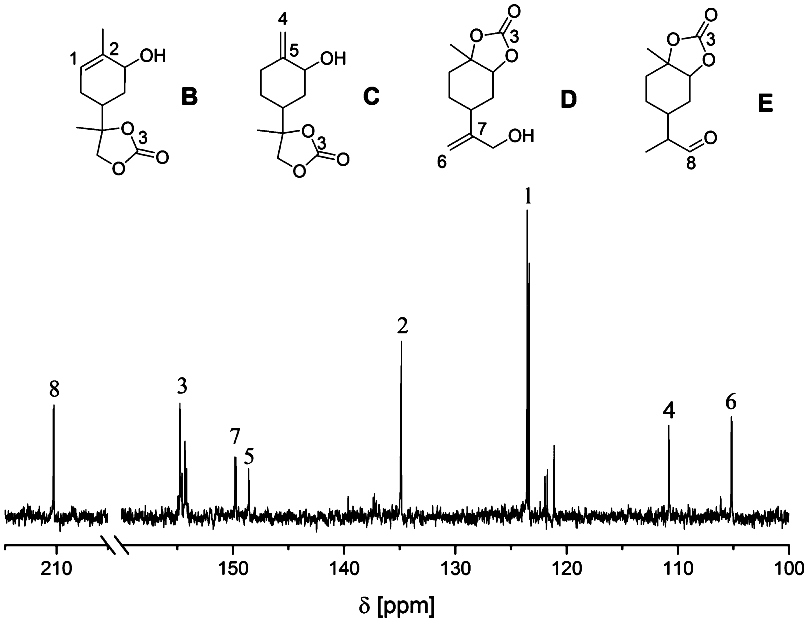

Figure 3. ^{13}C NMR spectrum ($CDCl_3$) of crude LC prior to purification shows various olefin signals corresponding to byproducts **B** to **D** and a carbonyl signal corresponding to the aldehyde byproduct **E**.

purification.[17] From their ^{1}H NMR spectra of the unpurified reaction products it is clearly visible that the higher temperature affords olefinic side products, although this side reaction is not mentioned.

Grown from solution single crystals of *trans*-LC with sizes up to 4 mm were obtained (see Figure 4b), enabling analysis of the LC crystal structure by X-ray diffraction (Supporting Information; pp S45−S48). As illustrated in Figure 4a, *trans*-LC crystallizes in the chiral orthorhombic space group $P2_12_12_1$ (no. 19), having the cell constants a = 8.1730(3) Å, b = 10.8726(4) Å, and c = 13.4157(5) Å with one molecule in the asymmetric unit and four molecules per unit cell. The structure refined to an R_1 of 2.68%, a wR_2 of 7.22%, and a Parsons parameter of −0.04(9), thereby confirming the absolute structure and the absolute configuration of the isolated isomer.

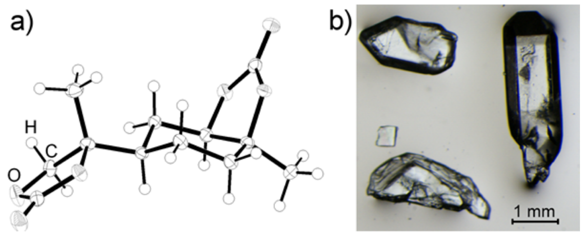

Figure 4. (a) Structure of *trans*-LC determined from single-crystal X-ray diffraction. (b) Single crystals of *trans*-LC grown from isohexane and ethyl acetate.

Figure 5 shows the calorimetric analysis of precipitated LC with 95% purity, which melts at 113 °C and does not recrystallize under given conditions. Whereas large amounts of impurities completely prevent crystallization, as seen in the direct carbonization product before purification (see Figure 1, left), small amounts impurities still lower melting temperature. The high purity LC blend of both stereoisomers showed a broad melting range between 105 and 160 °C while little recrystallization occurred during second heating. The melting range showed two maxima, at 122 and 157 °C, each corresponding to one stereoisomer. In sharp contrast, the pure *trans*-LC exhibited higher melting temperature at 165 °C. During second heating of the pure LC isomer a significant amount of recrystallization occurred (see Figure 5). Obviously, LC side-products and the presence of more than one diasteromer impair crystallization.

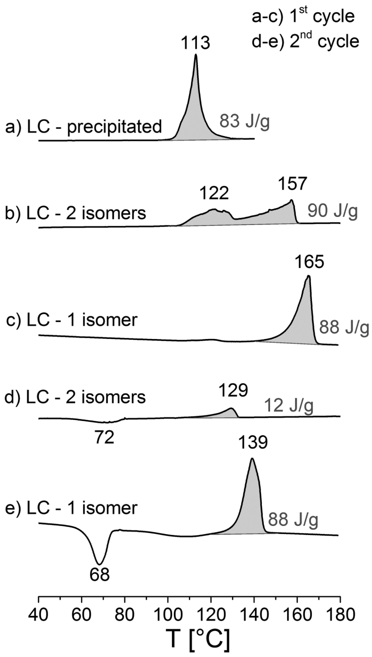

Figure 5. DSC traces (10 K/min) of precipitated LC (a, 95% purity), high purity LC blend (b, d) of two stereoisomers, and pure *trans*-LC (c, e).

Synthesis of Linear LC-Based NIPU Homo- and Copolymers. It is generally known that during the amine-mediated ring-opening of five-membered cyclic carbonates (5mcc) alkylation side reactions become increasingly significant at temperatures above 130 °C. Taking into account the high

DOI: 10.1021/acs.macromol.6b02460

Table 1. Reaction Conditions, Molar Masses, and Thermal Properties of Linear NIPU Thermoplastics

product	m_f (LC) [wt %]	t [h]	T [°C]	M_n[a] [kg/mol]	M_w[a] [kg/mol]	PDI	T_g[b] [°C]
BDGC_PA		5/5	100/120	22.1	46.7	2.1	−18
BDGC^3-LC^1_PA[c]	7.8	15; 18	130; 120	12.2	26.5	2.2	−10
BDGC^1-LC^1_PA[c]	16.9	20; 9	130; 120	10.7	21.8	2.0	−1
BDGC^2-LC^3_PA[c]	21.3	48; 20	130; 120	10.6	22.8	2.1	5
LC_PA	32.4	143	130	4.3	8.1	1.9	11

[a] SEC (DMAc, RT, PMMA). [b] DSC (10 K/min, second heating curve). [c] Preparation in two steps: LC-prepolymer formation and subsequent polymerization with BDGC. The exponents indicate the molar ratio of BDGC and LC.

Scheme 3. Side-Reactions Found When LC Reacted with 1-Octylamine (OA) in Boiling Chloroform for 4 days[a]

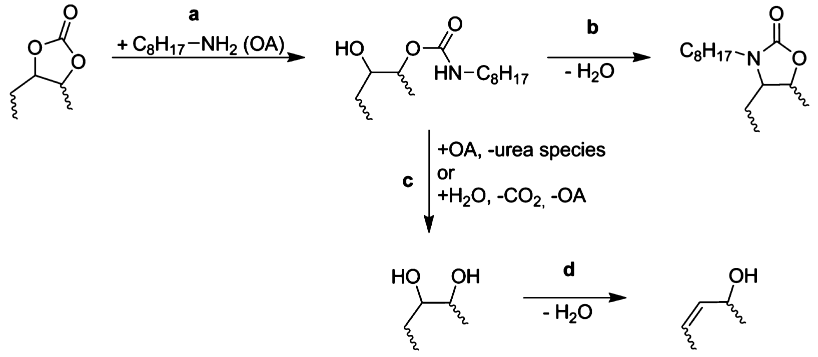

[a] Pathway **a** shows the formation of the hydroxy urethane group which can subsequently dehydrate (pathway **b**) to form a cyclic carbamate. Aminolysis or hydrolysis of the urethane group can lead to the formation of diols (pathway **c**). The subsequent elimination of water affords olefinic species (pathway **d**).

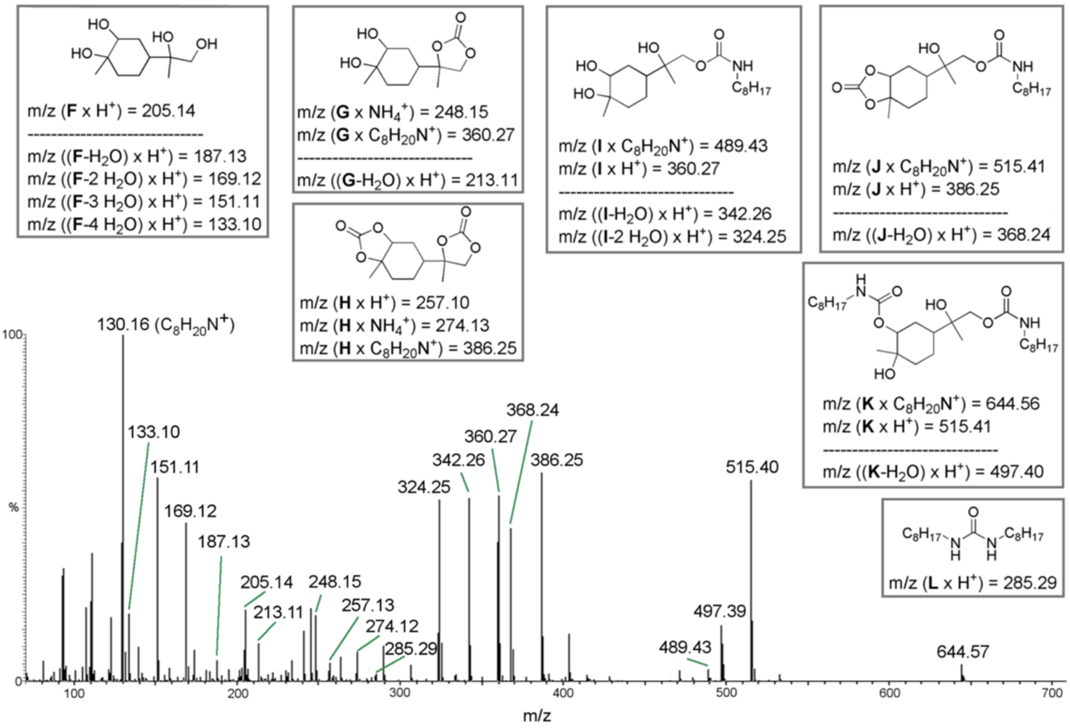

Figure 6. Mass spectrum (APCI) and the signal assignment of the products obtained when LC reacted with 1-octylamine in boiling chloroform for 4 days.

melting temperature of pure LC blend and the rather low reactivity of its electron-rich endocyclic 5mcc, LC polyaddition in bulk and the absence of catalysts requires elevated reaction temperatures. The bio-based high molecular mass diamine Priamine 1074 (PA), commercially available and derived from dimer−fatty acid, was used to prepare linear NIPU by LC-mediated polyaddition at 130 °C under nitrogen. Under these reaction conditions LC did not melt completely. Yet higher temperatures are likely to cause alkylation. Once a homogeneous mixture was obtained after a couple of hours, amine and cyclic carbonate consumptions were monitored by means of ^{1}H NMR and IR spectroscopy. LC_PA showed residual amine

(Figure S11, at 2.65 ppm) and cyclic carbonate groups (Figure S36, at 1801 cm^{-1}) even after almost 6 days at 130 °C, which was attributed to the low reactivity of the endocyclic 5mcc. Besides the stoichiometric 1 mol/1 mol ratio of functional groups, also excess PA was employed to prepare lower molar mass LC prepolymers containing two amine end groups. Full conversion of all cyclic carbonates was achieved within 15−48 h, indicated by the disappearance of the cyclic carbonate absorption band in the respective IR spectrum. Then difunctional carbonated 1,4-butanediol diglycidyl ether (BDGC), having much higher reactivity, was added to afford molar mass buildup by means of the BDGC-mediated chain extension reaction (see Scheme 1). Three copolymers with variable LC contents, together with the BDGC_PA and LC_PA homopolymers, were prepared in order to examine the influence of LC incorporation on NIPU properties.

As for the thermal properties, the results of the calorimetric analysis in Table 1 revealed a significant increase of glass transition temperatures with increasing LC content. This is attributed to the incorporation of the rather rigid LC units into the NIPU backbone. However, the polymer molar masses drastically decreased with increasing LC content. Whereas the BDGC_PA homopolymer exhibited high weight-average molar mass of M_w of 46.7 kg/mol, the incorporation of 7.8 wt % LC was sufficient to lower M_w to 26.5 g/mol. At higher content of 32.4 wt %, the molar mass was further reduced to 8.1 kg/mol. This finding presents strong experimental evidence for LC-mediated side reactions impairing stoichiometry.

Recent publications have already addressed the role of side-reactions in NIPU synthesis.[47,48] Typically, side-reactions like alkylation yielding *β*-hydroxyamines or cyclization of the *β*-hydroxyurethane group forming a cyclic carbamate may alter the polymer backbone but do not terminate the growing chain. In contrast, the aminolysis of urethane groups forming urea groups together with diols represents a prominent example of side reactions which drastically disrupts stochiometry.[47,48] Mass spectrometric studies of NIPU formation, to the best of our knowledge, have focused exclusively on terminal cyclic carbonates. Opposite to cyclic carbonates containing terminal 5mcc groups with electron-withdrawing substitution, LC is considerably less reactive since it is relatively electron-rich and sterically hindered. In a model study LC was reacted with two equivalents of 1-octylamine for 4 days in refluxing chloroform. The reaction in solution was preferred over a bulk reaction as most monoamines exhibit high vapor pressure and long reaction times would lead to significant loss of amine. Afterward, the chloroform was stripped off in a vacuum, and the resulting reaction product was analyzed by means of NMR spectroscopy and mass spectrometry (APCI). Scheme 3 shows the side reactions found in this model reaction, and Figure 6 displays the mass spectrum of the reaction mixture together with the assigned structures.

Since the conversion was incomplete, as also determined by the ^{1}H NMR spectrum, the strong signal of unreacted octylamine is clearly visible in the mass spectrum (*m*/*z* 130.16). During ionization process the molecules form adducts with protons (M x H$^+$), ammonium (M x NH$^+$), or octylammonium (M x $C_8H_{20}N^+$). The latter leads to a difficulty in assigning the signals as some masses can belong to different structures (e.g., **H** x $C_8H_{20}N^+$ and **J** x H$^+$). Under these rather mild reaction conditions, no alkylation side products were detected. However, besides the expected presence of cyclic carbonate and urethane groups, a number of diol and dehydration products were identified. According to reports in the literature,[47] the formation of diol species during ring-opening aminolysis of cyclic carbonates occurs through aminolysis of already existing urethane groups, thus yielding the diol together with a urea species **L**, which appeared as a relatively small peak in the mass spectrum. The authors therefore presume the existence of another mechanism of the diol formation, namely, the hydrolysis of the urethane groups under alkaline conditions. The dehydration of hydoxy urethanes, yielding cyclic carbamates, has been reported by Besse et al.[47] Interestingly, for all the structures shown in Figure 6 (except for **H**) dehydration products were found, even for those that do not contain any hydroxyurethane groups (**F** and **G**; **I** shows 2-fold dehydration in spite of the presence of only one hydroxyurethane group). The elimination of water is catalyzed by alkaline conditions and in the case of diol species affords olefinic groups which are relatively stable due to their multiple alkyl substitution. In some cases subsequent tautomerization affords aldehyde or ketone groups, thus rendering the assignment of the corresponding structures more difficult. Because of relatively mild conditions and incomplete turnover the relatively small amounts of the urea and olefinic species could not be detected in either the ^{1}H or ^{13}C NMR spectrum (Figures S12, S22, and S23) of the model reaction product.

Figure 7 shows the ^{13}C NMR-HSQC spectrum of LC_PA. Signals 1 and 7 were assigned to residual amine ($-CH_2-NH_2$) and the endocyclic 5mcc group, respectively. Signal 2 corresponds to the methylene group next to the urethane-N. Signals 4 and 3 correspond to the primary and secondary alcohol, respectively, which may be either part of the hydroxyurethane or the diol group. It shall be noted that signal 4 does not appear in the spectrum of the model reaction LC_OA (Figure S23). Signals 5 and 8 most likely correspond to the methylene and methine groups next to the urethane-O, respectively. Signal 9, barely visible in the ^{13}C NMR spectrum and hidden in the broad −OH signal of the ^{1}H NMR spectrum,

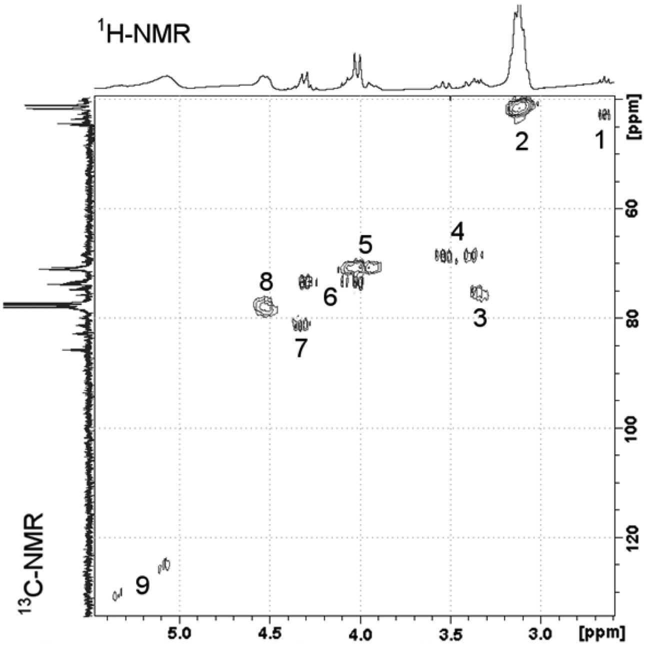

Figure 7. Two-dimensional ^{13}C NMR-HSQC spectrum of LC_PA.

verifies the existence of olefinic groups formed by dehydration reactions and thereby confirms the results of the mass spectrometric study of the model reaction LC_OA. Signal 6, with an AX spin system, is assigned to the methylene group of the cyclic carbamate. No urea species are detected.

Syntheses of 100% Bio-Based NIPU Thermosets. While ensuring the precise stoichiometry is crucial for the synthesis of high molar mass linear NIPU, it is considerably less relevant for cross-linking and formation of NIPU thermosets. The incorporation of rather rigid LC building blocks is of special interest with respect to boosting NIPU stiffness, especially when aiming at the development of 100% bio-based, "green" polyurethane coatings without requiring the addition of epoxy resins. For this purpose carbonated pentaerythritol glycidyl ether (PGC) was blended together with 10, 20, 30, and 50 wt % LC and cured with 1,5-diaminopentane (DAP), which is available by decarboxylation of lysine. The resulting DMA test specimens are shown in Figure 8a. Clearly, with increasing content of LC the corresponding NIPU thermoset turns out to be less colored. Furthermore, the cyclic carbonate groups of LC are considerably less reactive with respect to those of PGC. Lower LC reactivity accounts for longer pot lifetime, which is advantageous with respect to less demanding processing, but also reduces cure speed. Table 2 summarizes the results of the thermal and mechanical analyses of NIPU thermosets containing variable amounts of LC. With increasing LC content, glass transition temperatures gradually increased from 41 °C for PGC_DAP up to 62 °C for PGC-50LC_DAP comprising a PGC/LC (50/50) blend.

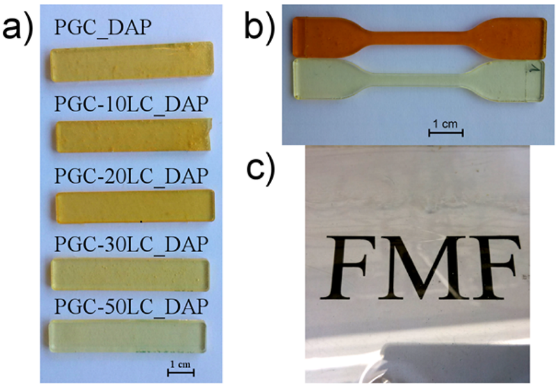

Figure 8. (a) DMA test specimens (80 × 12 × 3 mm) of PGC-LC_DAP thermosets containing variable amounts of purified LC. (b) LC_PEI tensile test specimens (5A) containing crude impure-LC (top) and purified LC (bottom). (c) LC_PEI coating (0.5 mm thickness) on a glass plate which was mounted on printed paper displaying the FMF logo.

Tensile testing revealed a significant increase of stiffness with increasing LC content in NIPU formulations, as reflected by substantial gains of Young's modulus. Albeit the average carbonate functionality gradually decreased with increasing the content of difunctional LC relative to polyfunctional PGC, the addition of 30 wt % LC increased tensile strength by 26% from 70 ± 2 to 88 ± 4 MPa. However, a drastic decay of tensile strength occurred at higher LC content of 50 wt %, paralleled by severe embrittlement and premature mechanical failure. Obviously, at low contents LC is highly attractive with respect to stiffening NIPU thermosets without sacrificing elongation at break.

In order to examine the role of LC purity regarding color formation, following procedure reported in the literature[31] for nonpurified LC, LC was cured with the polyfunctional polyethylene imine (PEI) Lupasol FG from BASF using either crude LC (impure-LC_PEI, Figure 8b, top) and purified LC (LC_PEI). Opposite to purified LC, crude LC accounted for severe color formation, as is clearly visible in Figure 8b by the dark brownish color of impure-LC_PEI containing nonpurified LC whereas purified LC caused significantly less color formation in castings (see Figure 8b). As is apparent from Figure 8c, thin LC_PEI coatings with thickness of 500 μm, prepared by curing purified LC with PEI, are fully transparent and colorless. Moreover, such NIPU coatings exhibit high gloss (140 ± 5). In addition to much less color formation, the purification of LC significantly improved thermal and mechanical properties of NIPU thermosets prepared by curing either crude LC or purified LC with PEI. Table 3 compares the state-of-the-art LC_PEI described by Bähr et al.[31] with the NIPU prepared by curing PEI with purified LC. Whereas nonpurified LC gave rather brittle NIPU thermosets, using purified LC accounted for higher glass temperature, which increased by 39 K from 55 to 94 °C, together with an almost 2-fold increased stiffness, as expressed by increasing the Young's

Table 3. Comparison of Thermal and Mechanical Properties of NIPU Thermosets LC_PEI Cured with State-of-the-Art Crude LC[31] and Purified LC

material	T_g[a] [°C]	T_g(tan δ)[b] [°C]	Young's modulus[c] [MPa]	σ_B[c] [MPa]	ε_B[c] [%]
impure-LC_PEI[d]		55 ± 5	2400 ± 700	7 ± 2	1 ± 1
LC_PEI[e]	80	94 ± 2	4370 ± 130	53 ± 5	1.29 ± 0.12

[a] DSC (10 K/min, second cycle). [b] DMA (3 K/min, 0.1%, 1 Hz), T_g determined from the maximum of the tan δ. [c] Tensile testing (ISO 527-1/2_5A, 5 mm/min, 5–6 specimens). [d] State-of-the-art LC by Bähr et al.[31] cured with PEI (10 h at 70 °C, 3 h at 100 °C). [e] Purified LC cured with PEI (16 h at 100 °C).

Table 2. Thermal and Mechanical Properties of Fully Bio-Based NIPU Thermosets Based on Various PGC/LC Mixtures and DAP

NIPU	m_f(LC) [wt %]	m_f(LC) [wt %]	T_g[a] [°C]	Young's modulus[b] [MPa]	σ_B[b] [MPa]	ε_B[b] [%]
PGC_DAP		0	41	3390 ± 120	70 ± 2	2.51 ± 0.12
PGC_10LC_DAP	7.78	8	45	3860 ± 50	83 ± 9	2.8 ± 0.5
PGC_20LC_DAP	15.6	16	48		not measured	
PGC_30LC_DAP	23.2	23	58	4040 ± 60	88 ± 4	2.49 ± 0.11
PGC_50LC_DAP	37.7	37	62		too brittle to measure	

[a] DSC (10 K/min, second cycle). [b] Tensile testing (ISO 527-1/2_5A, 5 mm min^{-1}).

DOI: 10.1021/acs.macromol.6b02460

modulus from 2400 to 4370 MPa, and accompanied by a 7.5-fold increase of tensile strength at break (σ_B) without affecting elongation at break.

CONCLUSION

Purification of limonene dicarbonate (LC), prepared by oxidation and subsequent carbonation of limonene, gained from orange peels, significantly improves thermal and mechanical properties of 100% bio-based non-isocyanate polyurethane (NIPU) materials. Moreover, it prevents the severe color formation typical for state-of-the-art LC-based NIPUs, thus for the first time enabling the use of LC in coating applications. According to NMR and mass spectrometric studies so far unknown olefinic side products are formed during tetrabutylammonium bromide (TBAB)-catalyzed carbonation of limonene dioxide. Because of these impurities the crude reaction product is received as a viscous liquid with dark red color, while LC purified by crystallization is a colorless crystalline solid. To date, only the crude LC carbonization product was applied in NIPU synthesis, and the comparison with purified LC, cured with flexible polyfunctional amines such as polyethylenimine (PEI), demonstrates that purified LC prevents color formation and significantly improves glass temperature (+39 K), stiffness (+82%), and tensile strength (+660%) of the resulting LC/PEI NIPU. In fact, small amounts of purified LC are sufficient to improve stiffness of various NIPU thermosets without affecting elongation at break. For 100% bio-based NIPUs, prepared by curing the carbonated pentaerythritol glycidyl ether PGC/LC blend with bio-based 1,5-diaminopentane (DAP), the addition of 23 wt % LC is sufficient to increase the glass temperature by 17 °C, paralleled by increasing the tensile strength from 70 to 88 MPa and the Young's modulus from 3390 to 4040 MPa while maintaining the elongation at break at 2.5%. Embrittlement observed at 37.7 wt % is attributed to the high rigidity of the LC units and lower cross-link density with increasing LC content.

Purified LC also enables to increase stiffness and molar mass of linear NIPUs which are of interest regarding the preparation of reactive NIPU prepolymers, NIPU thermoplastics, and thermoplastic NIPU elastomers containing alternating rigid LC-based hard segments and elastomeric segments. For example, polyaddition of high purity LC with flexible dimer-acid-based diamine (Priamine 1074) affords diamine-terminated prepolymers which are readily chain extended with the more reactive difunctional carbonated 1,4-butanediol diglycidyl ether (BDGC) to produce linear NIPU copolymers. However, NIPU molar mass declines with increasing LC content. According to the spectroscopic investigations of the model reaction of LC with octylamine, this is attributed to side reactions such as diol and olefin formation, which terminate the polymer chain and impair stoichiometry required for achieving higher molar mass of linear NIPUs. Obviously, during LC synthesis as well as during LC polymerization, olefin-forming side reactions indicate that LC has a tendency to fall back into its underlying terpene structure. More research is required to study the role of catalysts, which may accelerate polymerization and reduce side reactions. Since NIPU thermosets are less sensitive to such minor variations of stoichiometry, high purity LC represents a versatile building block for tailoring 100% bio-based NIPU thermosets which employ LC as highly efficient stiffening agent. Furthermore, this massively reduced color formation in conjunction with high stiffness and high gloss is of particular interest with respect to exploiting high purity LC in NIPU coating applications.

ASSOCIATED CONTENT

Supporting Information

The Supporting Information is available free of charge on the ACS Publications website at DOI: 10.1021/acs.macromol.6b02460.

^{1}H and ^{13}C NMR, FTIR, and mass spectra, stoichiometric ratios, calculations, SEC, TGA, tensile testing, DMA and DSC graphs, crystallographic data (PDF)

AUTHOR INFORMATION

Corresponding Author

*E-mail: rolfmuelhaupt@web.de (R.M.).

ORCID

Vitalij Schimpf: 0000-0002-9232-0479

Notes

The authors declare no competing financial interest.

ACKNOWLEDGMENTS

The authors gratefully acknowledge financial support of the Baden-Württemberg Stiftung (BioMatS-02). Marina Hagios, Alfred Hasenhindl, Christoph Warth, Julia Hettenbach, and Dr. Victor Hugo Pacheco Torres are acknowledged for their technical support. Donations of Priamine 1074 by Croda GmbH, Lupasol FG by BASF as well as ERISYSTM GE-21 from CVC emerald materials and ipox LC 16 from ipox chemicals are gratefully acknowledged.

ABBREVIATIONS

5mcc, 5-membered cyclic carbonate; LC, limonene dicarbonate; BDGC, carbonated 1,4-butanediol diglycidyl ether; PGC, carbonated pentaerythritol glycidyl ether; PA, Priamine 1074; EEW, epoxy equivalent weight.

REFERENCES

(1) Bayer, O. Das Di-Isocyanat-Polyadditionsverfahren (Polyurethane). *Angew. Chem.* **1947**, *59*, 257−272.

(2) PlasticsEurope. An analysis of European plastics production, demand and waste data. Plastics – the Facts 2014/2015, 2015.

(3) Dieterich, D. Polyurethane - nach 50 Jahren immer noch jung. *Chem. Unserer Zeit* **1990**, *24*, 135−142.

(4) Langanke, J.; Wolf, A.; Hofmann, J.; Böhm, K.; Subhani, M. A.; Müller, T. E.; Leitner, W.; Gürtler, C. Carbon dioxide (CO 2) as sustainable feedstock for polyurethane production. *Green Chem.* **2014**, *16*, 1865−1870.

(5) Blattmann, H.; Fleischer, M.; Bähr, M.; Mülhaupt, R. Isocyanate- and phosgene-free routes to polyfunctional cyclic carbonates and green polyurethanes by fixation of carbon dioxide. *Macromol. Rapid Commun.* **2014**, *35*, 1238−1254.

(6) Rokicki, G.; Parzuchowski, P. G.; Mazurek, M. Non-isocyanate polyurethanes: Synthesis, properties, and applications. *Polym. Adv. Technol.* **2015**, *26*, 707−761.

(7) Rokicki, G. Aliphatic cyclic carbonates and spiroorthocarbonates as monomers. *Prog. Polym. Sci.* **2000**, *25*, 259−342.

(8) Yu, T.; Weiss, R. G. Syntheses of cyclic carbonates with amidinium halide catalysts in reusable, reversible, room-temperature ionic liquids or acetonitrile. *Green Chem.* **2012**, *14*, 209−216.

(9) Takahashi, T.; Watahiki, T.; Kitazume, S.; Yasuda, H.; Sakakura, T. Synergistic hybrid catalyst for cyclic carbonate synthesis: remarkable acceleration caused by immobilization of homogeneous catalyst on silica. *Chem. Commun. (Cambridge, U. K.)* **2006**, 1664−1666.

(10) Guan, J.; Song, Y.; Lin, Y.; Yin, X.; Zuo, M.; Zhao, Y.; Tao, X.; Zheng, Q. Progress in Study of Non-Isocyanate Polyurethane. *Ind. Eng. Chem. Res.* **2011**, *50*, 6517−6527.

(11) Takeda, N.; Inoue, S. Polymerization of 1,2-Epoxypropane and Copolymerization with Carbon Dioxide Catalyzed by Metalloporphyrins. *Makromol. Chem.* **1978**, *179*, 1377−1381.

(12) Cokoja, M.; Bruckmeier, C.; Rieger, B.; Herrmann, W. A.; Kuhn, F. E. Transformation of carbon dioxide with homogeneous transition-metal catalysts: a molecular solution to a global challenge? *Angew. Chem., Int. Ed.* **2011**, *50*, 8510−8537.

(13) Clegg, W.; Harrington, R. W.; North, M.; Pasquale, R. Cyclic carbonate synthesis catalysed by bimetallic aluminium-salen complexes. *Chem. - Eur. J.* **2010**, *16*, 6828−6843.

(14) Decortes, A.; Castilla, A. M.; Kleij, A. W. Salen-complex-mediated formation of cyclic carbonates by cycloaddition of CO_2 to epoxides. *Angew. Chem., Int. Ed.* **2010**, *49*, 9822−9837.

(15) Barkakaty, B.; Morino, K.; Sudo, A.; Endo, T. Amidine-mediated delivery of CO 2 from gas phase to reaction system for highly efficient synthesis of cyclic carbonates from epoxides. *Green Chem.* **2010**, *12*, 42−44.

(16) Jiang, H.-F.; Yuan, B.-Z.; Qi, C.-R. Coupling of Carbon Dioxide with Epoxides Catalyzed by Amino Acid Hydrochloride Salts. *Chin. J. Chem.* **2008**, *26*, 1305−1308.

(17) Fiorani, G.; Stuck, M.; Martin, C.; Belmonte, M. M.; Martin, E.; Escudero-Adan, E. C.; Kleij, A. W. Catalytic Coupling of Carbon Dioxide with Terpene Scaffolds: Access to Challenging Bio-Based Organic Carbonates. *ChemSusChem* **2016**, *9*, 1304−1311.

(18) Nishikubo, T.; Kameyama, A.; Yamashita, J.; Tomoi, M.; Fukuda, W. Insoluble polystyrene-bound quaternary onium salt catalysts for the synthesis of cyclic carbonates by the reaction of oxiranes with carbon dioxide. *J. Polym. Sci., Part A: Polym. Chem.* **1993**, *31*, 939−947.

(19) Sakakura, T.; Kohno, K. The synthesis of organic carbonates from carbon dioxide. *Chem. Commun. (Cambridge, U. K.)* **2009**, 1312−1330.

(20) Du, Y.; Cai, F.; Kong, D.-L.; He, L.-N. Organic solvent-free process for the synthesis of propylene carbonate from supercritical carbon dioxide and propylene oxide catalyzed by insoluble ion exchange resins. *Green Chem.* **2005**, *7*, 518.

(21) Kihara, N.; Endo, T. Synthesis and properties of poly(hydroxyurethane)s. *J. Polym. Sci., Part A: Polym. Chem.* **1993**, *31*, 2765−2773.

(22) Ochiai, B.; Kojima, H.; Endo, T. Synthesis and properties of polyhydroxyurethane bearing silicone backbone. *J. Polym. Sci., Part A: Polym. Chem.* **2014**, *52*, 1113−1118.

(23) Ochiai, B.; Satoh, Y.; Endo, T. Nucleophilic polyaddition in water based on chemo-selective reaction of cyclic carbonate with amine. *Green Chem.* **2005**, *7*, 765.

(24) Kim, M.-R.; Kim, H.-S.; Ha, C.-S.; Park, D.-W.; Lee, J.-K. Syntheses and thermal properties of poly(hydroxy)urethanes by polyaddition reaction of bis(cyclic carbonate) and diamines. *J. Appl. Polym. Sci.* **2001**, *81*, 2735−2743.

(25) Mooney, J.; Valentine, C.; Rathke, T.; Svenson, D. Patent US20130030067: Sugar-Based Polyurethanes, Methods for Their Preparation, and Methods of Use Thereof; https://www.google.com/patents/US20130030067.

(26) Fidalgo, D. M.; Kolender, A. A.; Varela, O. Stereoregular poly-O -methyl [m,n]-polyurethanes derived from D -mannitol. *J. Polym. Sci., Part A: Polym. Chem.* **2013**, *51*, 463−470.

(27) Prömpers, G.; Keul, H.; Höcker, H. Polyurethanes with pendant hydroxy groups: Polycondensation of 1,6-bis-O-phenoxycarbonyl-2,3:4,5-di-O-isopropylidenegalactitol and 1,6-di-O-phenoxycarbonylgalactitol with diamines. *Green Chem.* **2006**, *8*, 467−478.

(28) Besse, V.; Auvergne, R.; Carlotti, S.; Boutevin, G.; Otazaghine, B.; Caillol, S.; Pascault, J.-P.; Boutevin, B. Synthesis of isosorbide based polyurethanes: An isocyanate free method. *React. Funct. Polym.* **2013**, *73*, 588−594.

(29) Boyer, A.; Cloutet, E.; Tassaing, T.; Gadenne, B.; Alfos, C.; Cramail, H. Solubility in CO_2 and carbonation studies of epoxidized fatty acid diesters: Towards novel precursors for polyurethane synthesis. *Green Chem.* **2010**, *12*, 2205.

(30) Javni, I.; Hong, D. P.; Petrović, Z. S. Polyurethanes from soybean oil, aromatic, and cycloaliphatic diamines by nonisocyanate route. *J. Appl. Polym. Sci.* **2013**, *128*, 566−571.

(31) Bähr, M.; Bitto, A.; Mülhaupt, R. Cyclic limonene dicarbonate as a new monomer for non-isocyanate oligo- and polyurethanes (NIPU) based upon terpenes. *Green Chem.* **2012**, *14*, 1447.

(32) Bähr, M.; Mülhaupt, R. Linseed and soybean oil-based polyurethanes prepared via the non-isocyanate route and catalytic carbon dioxide conversion. *Green Chem.* **2012**, *14*, 483.

(33) Unverferth, M.; Kreye, O.; Prohammer, A.; Meier, M. A. R. Renewable non-isocyanate based thermoplastic polyurethanes via polycondensation of dimethyl carbamate monomers with diols. *Macromol. Rapid Commun.* **2013**, *34*, 1569−1574.

(34) Fleischer, M.; Blattmann, H.; Mülhaupt, R. Glycerol-, pentaerythritol- and trimethylolpropanebased polyurethanes and their cellulose carbonate composites prepared via the non-isocyanate route with catalytic carbon dioxide fixation. *Green Chem.* **2013**, *15*, 934.

(35) Cornille, A.; Dworakowska, S.; Bogdal, D.; Boutevin, B.; Caillol, S. A new way of creating cellular polyurethane materials: NIPU foams. *Eur. Polym. J.* **2015**, *66*, 129−138.

(36) Bähr, M.; Mühlhaupt, R.; Ritter, B. S. Patent WO2012171659A1: Carbonate group comprising terpene-derived monomers and isocyanate-free polyurethanes; https://google.com/patents/WO2012171659A1?cl=en&hl=de.

(37) Greenspan, F. P. Composition comprising epoxypolybutadiene and limonene diepoxide, US 3073792, 1963.

(38) Byrne, C. M.; Allen, S. D.; Lobkovsky, E. B.; Coates, G. W. Alternating copolymerization of limonene oxide and carbon dioxide. *J. Am. Chem. Soc.* **2004**, *126*, 11404−11405.

(39) Pena Carrodeguas, L.; Gonzalez-Fabra, J.; Castro-Gomez, F.; Bo, C.; Kleij, A. W. Al(III) -catalysed formation of poly(limonene)-carbonate: DFT analysis of the origin of stereoregularity. *Chem. - Eur. J.* **2015**, *21*, 6115−6122.

(40) Auriemma, F.; De Rosa, C.; Di Caprio, M. R.; Di Girolamo, R.; Ellis, W. C.; Coates, G. W. Stereocomplexed poly(limonene carbonate): a unique example of the cocrystallization of amorphous enantiomeric polymers. *Angew. Chem., Int. Ed.* **2015**, *54*, 1215−1218.

(41) Li, C.; Sablong, R. J.; Koning, C. E. Chemoselective Alternating Copolymerization of Limonene Dioxide and Carbon Dioxide: A New Highly Functional Aliphatic Epoxy Polycarbonate. *Angew. Chem., Int. Ed.* **2016**, *55*, 11572−11576.

(42) Vora, J. D.; Matthews, R. F.; Crandall, P. G.; Cook, R. Preparation and Chemical Composition of Orange Oil Concentrates. *J. Food Sci.* **1983**, *48*, 1197−1199.

(43) Coleman, R. L.; Lund, E. D.; Moshonas, M. G. Composition of Orange Essence Oil. *J. Food Sci.* **1969**, *34*, 610−611.

(44) Badee, A.; Helmy, S. A.; Morsy, N. F. Utilisation of orange peel in the production of α-terpineol by Penicillium digitatum (NRRL 1202). *Food Chem.* **2011**, *126*, 849−854.

(45) Braddock, R. J. *Handbook of Citrus By-products and Processing Technology*; John Wiley & Sons: New York, 1999.

(46) Annunziata, L.; Diallo, A. K.; Fouquay, S.; Michaud, G.; Simon, F.; Brusson, J.-M.; Carpentier, J.-F.; Guillaume, S. M. α,ω-Di(glycerol carbonate) telechelic polyesters and polyolefins as precursors to polyhydroxyurethanes: an isocyanate-free approach†. *Green Chem.* **2014**, *16*, 1947−1956.

(47) Besse, V.; Camara, F.; Méchin, F.; Fleury, E.; Caillol, S.; Pascault, J.-P.; Boutevin, B. How to explain low molar masses in PolyHydroxyUrethanes (PHUs). *Eur. Polym. J.* **2015**, *71*, 1−11.

(48) Lamarzelle, O.; Durand, P.-L.; Wirotius, A.-L.; Chollet, G.; Grau, E.; Cramail, H. Activated lipidic cyclic carbonates for non-isocyanate polyurethane synthesis. *Polym. Chem.* **2016**, *7*, 1439−1451.

(49) Demirbas, A. Biofuels sources, biofuel policy, biofuel economy and global biofuel projections. *Energy Convers. Manage.* **2008**, *49*, 2106−2116.

DOI: 10.1021/acs.macromol.6b02460
Macromolecules XXXX, XXX, XXX−XXX

(50) Krause, L.; Herbst-Irmer, R.; Sheldrick, G. M.; Stalke, D. Comparison of silver and molybdenum microfocus X-ray sources for single-crystal structure determination. *J. Appl. Crystallogr.* **2015**, *48*, 3−10.

(51) Sheldrick, G. M. SHELXT - integrated space-group and crystal-structure determination. *Acta Crystallogr., Sect. A: Found. Adv.* **2015**, *71*, 3−8.

(52) Sheldrick, G. M. Crystal structure refinement with SHELXL. *Acta Crystallogr., Sect. C: Struct. Chem.* **2015**, *71*, 3−8.

(53) Hubschle, C. B.; Sheldrick, G. M.; Dittrich, B. ShelXle: a Qt graphical user interface for SHELXL. *J. Appl. Crystallogr.* **2011**, *44*, 1281−1284.

(54) Parsons, S.; Flack, H. D.; Wagner, T. Use of intensity quotients and differences in absolute structure refinement. *Acta Crystallogr., Sect. B: Struct. Sci., Cryst. Eng. Mater.* **2013**, *69*, 249−259.

(55) Whiteoak, C. J.; Kielland, N.; Laserna, V.; Castro-Gomez, F.; Martin, E.; Escudero-Adan, E. C.; Bo, C.; Kleij, A. W. Highly active aluminium catalysts for the formation of organic carbonates from CO_2 and oxiranes. *Chem. - Eur. J.* **2014**, *20*, 2264−2275.